SECOND EUROPEAN CONFERENCE ON EARTHQUAKE ENGINEERING
AND SEISMOLOGY, ISTANBUL AUG. 25-29, 2014

NONLINEAR SEISMIC RESPONSE OF RC FRAMED STRUCTURES RETROFITTED BY DIFFERENT ISOLATION SYSTEMS

Alfonso VULCANO[1], Fabio MAZZA[2], Mirko MAZZA[3]

ABSTRACT

To check the effectiveness of different isolation systems for retrofitting a r.c. framed structure located in a near-fault area, a numerical investigation is carried out analyzing the nonlinear dynamic response of the fixed-base and isolated structures. The following base-isolation systems are considered, assuming different properties and in-plan layout: elastomeric bearings acting alone or, alternatively, combined in parallel or in series with sliding bearings; friction pendulum bearings. The different isolation systems are designed assuming the same value of the fundamental vibration period. R.c. frame members are idealized by a two-component model, assuming a bilinear moment-curvature law; the effect of the axial load on the ultimate bending moment of columns is taken into account. The response of an elastomeric bearing is simulated by a model with variable stiffness properties in the horizontal and vertical directions, depending on the axial force and lateral deformation; while the response of sliding and friction pendulum bearings is described by laws with friction variability, depending on deformation velocity and geometry. The nonlinear analysis of the fixed-base and isolated structures subjected to horizontal and vertical components of near-fault ground motions is performed checking plastic conditions at the potential critical sections of the girders and columns; critical conditions of the isolation systems are checked as well.

INTRODUCTION

Existing structures designed in compliance with old codes present in many cases a high seismic vulnerability and need retrofitting. For this purpose different strategies can be followed, e.g. enhancing the strength and/or ductility capacity or modifying in a suitable way the distribution of the structural properties (mass, strength, stiffness). But sometimes these strategies may require very expensive and complex works. Alternatively, it can be easier and less expensive to use new techniques, i.e. base isolation and/or supplemental damping, which aim to reducing the seismic effects limiting the input energy and/or enhancing the energy dissipation capacity.

In particular, the insertion of isolation bearings at the base of a structure subjected to an earthquake allows a considerable reduction of the horizontal loads transmitted to the superstructure (Kelly, 1997). Elastomeric bearings (e.g. HDLRBs) lead to an increase of the fundamental vibration period of the structure, with a shift in the range of low spectral accelerations; frictional devices (e.g., steel-PTFE sliding bearings, SBs, or friction pendulum bearings, FPBs) lead to a limitation of the

[1] Full professor, Dipartimento di Ingegneria Civile, Università della Calabria, Rende (Cosenza), Italy, vulcano@unical.it
[2] Researcher, Dipartimento di Ingegneria Civile, Università della Calabria, Rende (Cosenza), Italy, fabio.mazza@unical.it
[3] Research Fellow, Dipartimento di Ingegneria Civile, Università della Calabria, Rende (Cosenza), Italy, mirko.mazza@unical.it

maximum force transmitted to the superstructure (Braga et al., 2005). As shown by Mazza and Vulcano (2009, 2012a, 2012b), in case of elastomeric bearings acting alone ("Base Isolation", BI, system) or combined in series with sliding bearings ("Base Isolation and in-Series Sliding", BISS, system), the structure tends to behave as isolated or fixed-base along the vertical direction depending on the value, respectively very low or very high, of the ratio α_{K0} between the vertical (K_{V0}) and horizontal (K_{H0}) nominal stiffnesses of the isolation system. Moreover, the behaviour of a "Base Isolation with in-Parallel Sliding" (BIPS) system in the vertical direction is expected similar to that of a fixed-base structure, providing the grid of girders placed above the isolation system with a high stiffness; while, the behaviour in a horizontal direction is like that of a fixed-base structure until the friction threshold imposed by the sliding bearings is not exceeded.

However, strong ground motions, especially near-fault ground motions which are characterized by long-duration horizontal pulses and high values of the ratio α_{PGA} between the peak value of the vertical acceleration (PGA_V) and the analogous value of the horizontal acceleration (PGA_H), can become critical for a base-isolated structure. More specifically, the horizontal deformability of a base-isolated structure may amplify the inelastic response of the superstructure and induce a failure of the isolation system (Mazza and Vulcano, 2009). Moreover, high values of α_{PGA} can notably modify the axial load in r.c. columns, while yielding is expected along the span of the girders, especially at the upper storeys (Mazza and Vulcano, 2012a, 2012b); in addition, elastomeric and sliding bearings can undergo tensile loads (Kasalanati and Constantinou, 2005) and uplifts (Ryan and Chopra, 2006), respectively.

The above considerations point out the importance of checking the effectiveness of different isolation systems for retrofitting a r.c. framed structure located in a near-fault area. For this purpose, a numerical investigation is carried out analyzing fixed-base (FB) and base-isolated structures with different properties and layout subjected to horizontal and vertical ground motions.

MODELING OF THE BASE-ISOLATION SYSTEMS

The base-isolation systems (e.g., see Naeim and Kelly, 1999) aim to carry the vertical loads (exhibiting a rather high vertical stiffness) and allow rather large horizontal displacements (exhibiting a low stiffness or strength in the horizontal direction). The large horizontal base displacement consequent to a near-fault ground motion can be enabled by oversizing the elastomeric bearings (e.g., increasing the geometric dimensions of the rubber layers) or increasing the roughness of the sliding surface of the frictional bearings. In alternative, the elastomeric bearing may act in parallel with a sliding bearing (e.g., the "Resilient-Friction Base Isolator", R-FBI) or in series with a sliding plate (e.g., the "Electricité de France" system, EDF) attached to its top or bottom surface. However, the BIPS system can increase the contribution of the higher vibration modes of the superstructure, while the BISS system is not always favourable in reducing the residual displacement of the isolation system (Mazza and Vulcano, 2012a and 2012 b).

The behaviour of the above illustrated base-isolation systems can be simulated by adopting the models shown in Figures 1a, 1b, 1c, 1d: exactly, Figures 1a and 1b refer, respectively, to elastomeric and frictional bearings; Figures 1c and 1d represent, respectively, BIPS and BISS systems. Whereas, a frictional pendulum bearing can be represented by the model in Figure 1e.

Elastomeric bearings (e.g., the high-damping-laminated-rubber-bearings, HDLRBs) provide energy dissipation and re-centring capability. Experimental results by Ryan et al. (2004) pointed out that the horizontal stiffness of a HDLRB (starting from K_{H0}) decreases with increasing vertical load (P), while the corresponding vertical stiffness (starting from K_{V0}) decreases with increasing lateral deformation (u_H).

To account for the observed behaviour, the two-spring-two-dashpot model shown in Figure 1a, constituted of a nonlinear spring acting in parallel with a linear viscous dashpot both in the horizontal and vertical directions, can be adopted (Mazza and Vulcano, 2012a and 2012 b). The nonlinear force-displacement laws for the horizontal (F_K-u_H) and vertical (P-u_V) springs are given as (Naeim and Kelly, 1999; Ryan et al., 2004)

$$F_K = K_H u_H = K_{H0}\left[1-\left(P/P_{cr}\right)^2\right] u_H \tag{1a}$$

$$P_K = K_V\left(u_V - \frac{\alpha_b}{\alpha_{K0}}\frac{16}{\pi^2\phi_b S_2}u_H^2\right) \tag{1b}$$

where the compressive or tensile critical load (P_{cr}) and the vertical stiffness (K_V) can be obtained according to experimental observations (Ryan et al., 2004) and, after some manipulations, can be specialized for a circular bearing of diameter ϕ_b as

$$P_{cr} = \pm\left(\pi\phi_b/4\right)K_{H0}\sqrt{\alpha_{K0}} \tag{2a}$$

$$K_V = K_{V0}\Big/\left[1+48\left(u_H/\pi\phi_b\right)^2\right] \tag{2b}$$

where $\alpha_b=h_b/t_r$, h_b and t_r being the total height of the bearing and the total thickness of the rubber, respectively (e.g., $\alpha_b=1.2$ can be considered as a mean value); $S_2=\phi_b/t_r$ is the secondary shape factor (e.g., $S_2\geq 4$ is a conservative assumption).

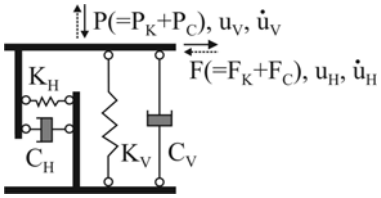

(a) Elastomeric bearing (e.g., HDLR bearing)

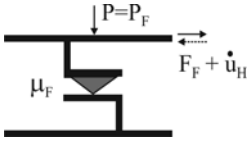

(b) Frictional bearing (e.g., steel-PTFE bearing)

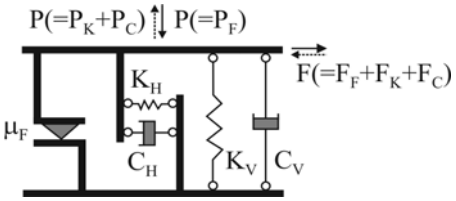

(c) In-parallel combination of elastomeric and sliding bearings (BIPS system: e.g., R-FBI)

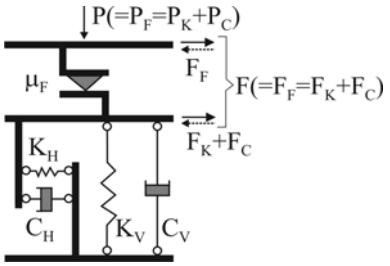

(d) In-series combination of elastomeric bearing and sliding plates (BISS system: e.g., EDF)

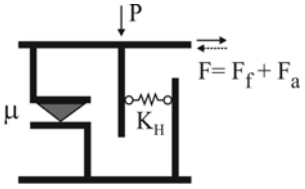

(e) Friction pendulum bearing

Figure 1. Modeling of base-isolation systems

Moreover, the linear force-velocity laws for the horizontal (F_C-$\dot{u}_H$) and vertical (P_C-$\dot{u}_V$) dashpots in Figure 1a are expressed as

$$F_C = C_H\dot{u}_H \cong \left(\xi_H K_{H0}T_{1H}/\pi\right)\dot{u}_H \tag{3a}$$

$$P_C = C_V\dot{u}_V \cong \left(\xi_V K_{V0}T_{1V}/\pi\right)\dot{u}_V \tag{3b}$$

where ξ_H (ξ_V) and T_{1H} (T_{1V}) represent the equivalent viscous damping ratio and the fundamental vibration period in the horizontal (vertical) direction, respectively. The response of a steel-PTFE sliding bearing (Figure 1b) basically depends on sliding velocity, contact pressure and temperature (e.g., Dolce et al., 2005). More specifically, the coefficient of sliding friction increases with increasing velocity up to a certain velocity value, beyond which it remains almost constant, while drops with increasing pressure (with a rate of reduction that is dependent on sliding velocity) and temperature.

The frictional force at the sliding interface can be expressed as

$$F_F = \mu_F \cdot P \cdot Z \tag{4a}$$

$$\mu_F = \mu_{max} - (\mu_{max} - \mu_{min}) \cdot e^{-\alpha \dot{u}_H} \tag{4b}$$

where Z is a dimensionless hysteretic quantity (Z takes values of ±1 during sliding and less then unity during sticking) and μ_F is the coefficient of friction at sliding velocity $\dot{u}_H$, which attains the value μ_{max} or μ_{min} respectively at high or very low velocity, while α is a constant for given values of pressure and temperature.

The nonlinear force-displacement (F-u_H) law of a friction pendulum bearing can be represented considering the restoring (F_r) and frictional (F_f) forces shown in Figure 1e:

$$F = F_r + F_f = (P/R)\, u_H + sign(\dot{u}_H)\, \mu P \tag{5}$$

where R, u_H and $\dot{u}_H$ represent, respectively, the radius of curvature of the sliding surface, the horizontal displacement and the velocity of the device, while P and μ are, respectively, the vertical load acting on the device and the friction coefficient (see Eq. (4b)).

DESIGN OF THE BASE-ISOLATED R.C. FRAMED STRUCTURES

Two r.c. framed structures are considered as fixed-base structures which need retrofitting.

The first one consists of a five-storey residential building (see plan in Figure 2a), which is supposed retrofitted by inserting at the base HDLRBs or, alternatively, a BISS or BIPS system (see elevation in Figure 2b).

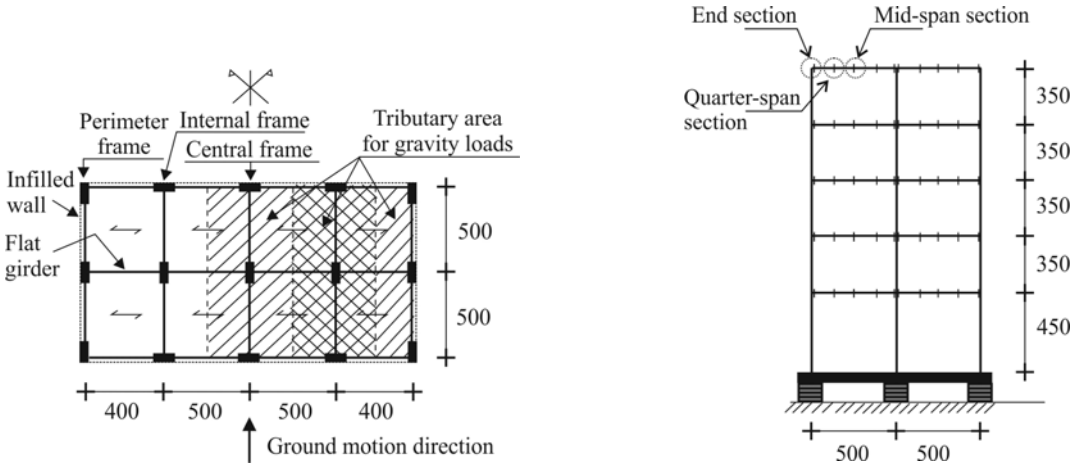

(a) Plan of the five-storey r.c. framed structure

(b) Elevation of an isolated five-storey frame structure

Figure 2. R.c. framed structure isolated at the base by HDLRBs, BISS or BIPS system (dimensions in cm)

The proportioning of the r.c. five-storey framed structure is done according to an old Italian seismic code (Legge n. 1684, 1962), assuming, besides the gravity loads, the horizontal seismic loads

as in a high-risk zone: seismic coefficient C=0.10 and design according to the allowable stress method. The gravity loads used in the design are represented by dead- and live-loads, respectively equal to: 4.3 kN/m^2 and 1 kN/m^2, for the top floor; 5 kN/m^2 and 2 kN/m^2, for the other floors. The contribution of the masonry-infills is taken into account considering a weight of 2.7 kN/m^2. The following masses are considered at each floor: lumped masses at the exterior and interior joints, in order to take into account the contribution of the transverse girders and, in case of the exterior joints, also the one of the masonry infills; uniformly distributed mass along the girders and columns, accounting for the gravity load of the structural member and, in the case of a girder, also for that of the floor slab and masonry infills (only for girders of perimeter frames). A cylindrical compressive strength of 25 N/mm^2 for concrete and a yield strength of 440 N/mm^2 for steel are assumed.

The design of the superstructure has been carried out satisfying some minimum conditions for the longitudinal bars of the girders and columns: at least two 14 mm bars are provided at the top and bottom throughout the length of all the frame members; for the girders, a tension reinforcement ratio not less than 0.31% (for the assumed yield strength) is provided and, at their end sections, a compression reinforcement not less than half of the tension reinforcement is placed; a minimum steel geometric ratio of 1% is assumed for the symmetrically-reinforced section of each column.

The isolation systems, which are supposed inserted at the base for retrofitting the r.c. framed structure, are designed according to the current Technical regulations for the constructions by the Italian Ministry of the Infrastructures (2008), labeled as NTC08, assuming, with reference to the horizontal and vertical seismic loads, the same value of the behaviour factor (i.e. $q_H=q_V=1.5$). Moreover, the following design assumptions are made: moderately soft soil (class D, subsoil parameters: $S_{SH}=1.45$ in the horizontal direction and $S_{SV}=1$ in the vertical one); flat terrain (class T1, topographic parameter: $S_T=1$); high-risk seismic region (peak ground acceleration in the horizontal, PGA_H, and vertical, PGA_V, directions equal to 0.404g and 0.278g, respectively).

Because of the structural symmetry and assuming the floor slabs infinitely rigid in their own plane, the entire structure of Figure 2 is idealized by an equivalent plane frame (pseudo-three-dimensional model) along the horizontal ground motion direction, whose elements have stiffness and strength properties so that the two perimeter (lateral) frames, the two interior frames and the central one could be represented as a whole (Mazza et al., 2012a and 2012b). The tributary mass resulting from the overall building and the gravity loads corresponding to the tributary area marked in Figure 2a are considered for each of them, assuming infilled walls placed along the perimeter of the building as non-structural elements regularly distributed in elevation. Cross-sections of the frame members are shown in Table 1.

Table 1. Cross sections of columns and girders for the five-storey r.c. framed structure in Figure 2a

Storey	Columns	Girders
5	30x30	30x45
4	30x40	30x50
3	30x50	30x55
2	30x60	30x60
1	30x65	30x65
base	-	40x100

Different in-plan combinations and configurations of elastomeric and sliding bearings are considered for the retrofitting of the five-storey framed building: elastomeric bearings only (i.e. BI configuration in Figure 3a: HDLRBs type 1, which are simply assumed with the same dimensions obtaining a larger torsional stiffness); in-parallel combinations of elastomeric (HDLRBs type 2) and sliding bearings (i.e. BIPS-A, BIPS-B and BIPS-C configurations in Figures 3b, 3c and 3d, respectively); in-series combinations of elastomeric (HDLRBs type 3) and sliding bearings (i.e. BISS-A, BISS-B and BISS-C configurations in Figures 3e, 3f and 3g, respectively, with sliding bearings in the same position adopted for the BIPS systems but placed in-series with HDLRBs type 1). Each arrangement of elastomeric and sliding bearings corresponds to a value of the nominal sliding ratio $\alpha_{S0}(=F_{S0}/F_{S0,max})$, defined, under gravity loads, as the global sliding force (F_{S0}) corresponding to an examined BIPS (Figures 3b, 3c and 3d) or BISS (Figures 3e, 3f and 3g) system divided by the maximum sliding force ($F_{S0,max}$); this latter one evaluated supposing that elastomeric and sliding

bearings (or plates) are placed under each column. Three values of the nominal stiffness ratio of the HDLRBs (i.e. α_{K0}=200, 800, 2000) are considered for the BI, BIPS-A and BISS-A structures, while α_{K0}=800 is assumed for the BIPS-B, BIPS-C, BISS-B and BISS-C structures. The base-isolated structures are designed assuming the same values of the fundamental vibration period in the horizontal direction (i.e. T_{1H}=2.5 s) and equivalent viscous damping ratios in the horizontal (i.e. ξ_H=10%) and vertical (i.e. ξ_V=5%) directions. Moreover, the equivalent viscous damping of the sliding bearings (ξ_{HS}) is calculated referring to the (horizontal) spectral displacement, considering the gravity loads and a sliding friction coefficient μ_F=0.03. For each isolated structure, the following data are considered: nominal values of the stiffness (α_{K0}) and sliding (α_{S0}) ratios; equivalent viscous damping of the elastomeric (ξ_{HI}) and sliding (ξ_{HS}) bearings, in the horizontal direction; diameter of the HDLRBs (ϕ_b) and corresponding primary (S_1) and secondary (S_2) shape factors; compression modulus of the rubber-steel composite bearing (E_c). Further details can be found in works by the authors cited above (Mazza et al., 2012a and 2012b).

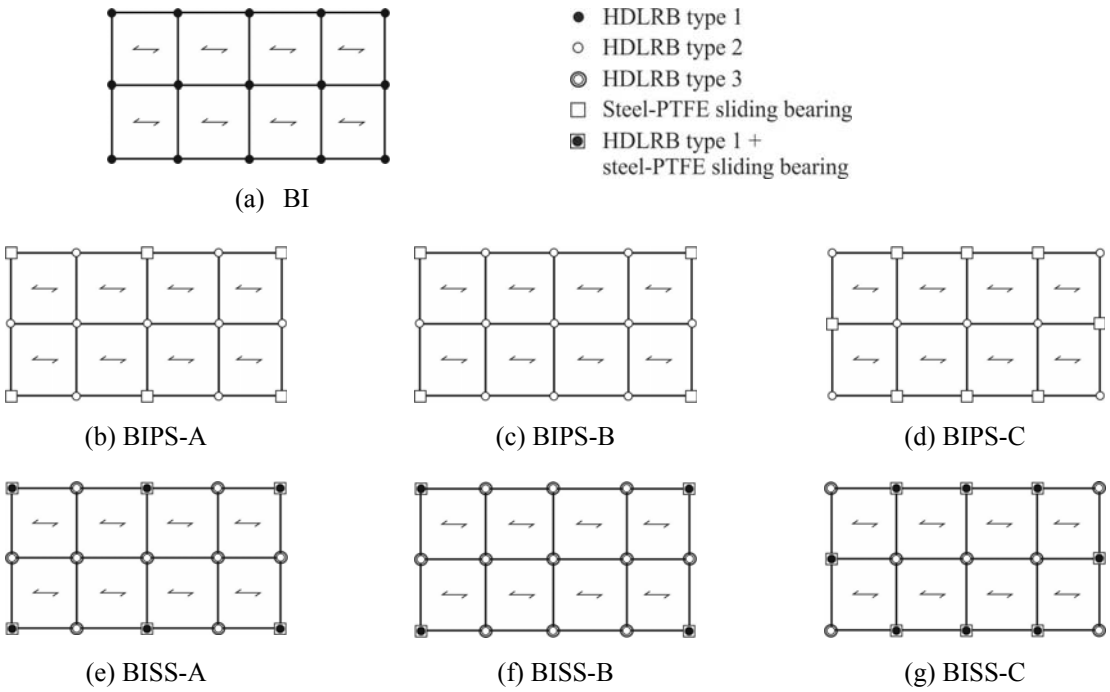

Figure 3. In-plan layout of the base-isolation systems

The design of the HDLRBs has been carried out according to the prescriptions imposed by NTC08, assuming a shear modulus of the elastomer G=0.35 MPa. In particular, the Ultimate Limit State (ULS) verifications regarding the maximum shear strains have been satisfied: i.e. $\gamma_{tot}=\gamma_s+\gamma_c+\gamma_\alpha\leq 5$ and $\gamma_s\leq 2$, where γ_{tot} represents the total design shear strain, while γ_s, γ_c and γ_α represent the shear strains of the elastomer due, respectively, to seismic displacement, axial compression and angular rotation. Moreover, the maximum compression axial load (P) has not exceeded the critical load (P_{cr}; see Eq. (2a)) divided by a safety coefficient equal to 2.0. Finally, the minimum tensile stress (σ_t) resulting from the seismic analysis has been assumed as 2G(=0.7 MPa) for all the elastomeric bearings. The design of the HDLRBs has been controlled by the condition imposed on the maximum shear strains (i.e. γ_{tot} and γ_α), with some exceptions for BI (i.e. for α_{K0}=200 and 800) and BISS-A (i.e. for α_{K0}=200) structures where the buckling control proved to be the more restrictive. No tensile axial loads were found.

The second r.c. framed structure considered in the present work is a six-storey residential building, which is supposed retrofitted by inserting at the base friction pendulum bearings (Figure 4). For this structure dead- and live-loads are assumed equal to those previously considered for the five-storey structure. Cross-sections of columns and girders are shown in Table 2.

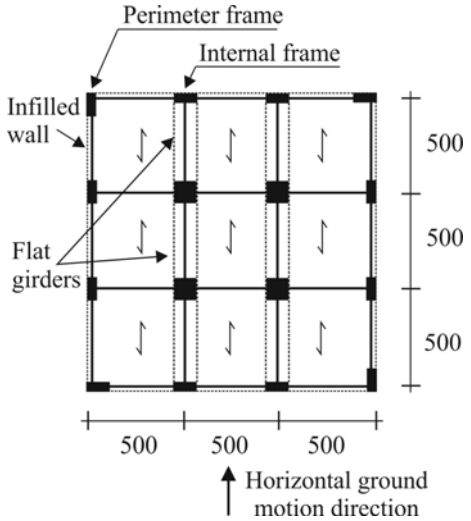

(a) Plan of the six-storey r.c. framed structure

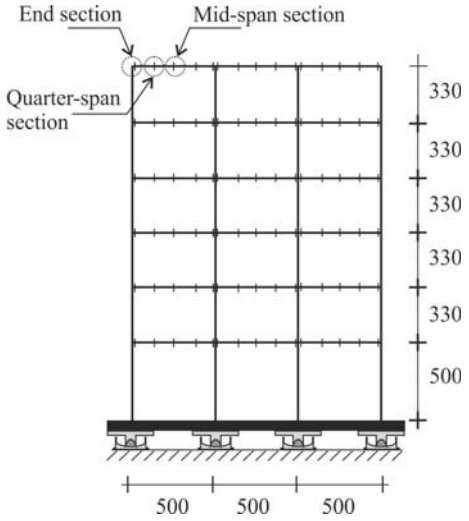

(b) Elevation of the isolated structure (along horizontal ground motion direction)

Figure 4. R.c. framed structure isolated at the base by friction pendulum bearings (dimensions in cm)

Table 2 - Cross sections of the r.c. frame members (see Figure 4)

(a) Columns

Storey	Corner columns	Central columns	Perimeter columns
6	30x50	40x40	30x50
5	30x50	40x40	30x50
4	30x60	50x50	40x60
3	30x60	50x50	40x60
2	40x70	60x60	50x80
1	40x70	60x60	50x80

(b) Girders

Storey	Deep girders	Flat girders
6	30x50	50x25
5	30x50	50x25
4	30x60	60x25
3	30x60	60x25
2	40x60	70x25
1	40x60	70x25
base	50x80	50x80

Three cases are considered for the base-isolated structure. The base friction pendulum bearings are designed assuming the same value of the fundamental vibration period in the horizontal direction (i.e. T_{1H}=2.5 s) and three values of the equivalent viscous damping ratio (i.e. ξ_H=10%, 20% and 30%). The radius of curvature (R) and friction coefficient (μ) of the bearings, which are supposed having the same dimensions, are evaluated by using the following equations (Calvi et al., 2010):

$$\mu = 2/\left(\pi + (\pi u_H)/(\mu R)\right) \tag{6a}$$

$$T_{1H} = 2\pi\left(g\left(1/R + \mu/u_H\right)\right)^{-1/2} \tag{6b}$$

where u_H represents the horizontal displacement evaluated as a function of the isolation period and equivalent viscous damping by using the design spectrum (see Table 3).

Table 3 – Properties of the friction pendulum bearings

Case	T_{1H}(s)	ξ_H(%)	R(m)	μ
1	2.5	10	1.84	0.025
2	2.5	20	2.25	0.038
3	2.5	30	2.94	0.048

NUMERICAL RESULTS

In order to check the effectiveness of the different isolation systems for retrofitting the two r.c. framed buildings considered in the previous Section, the nonlinear dynamic response of the fixed-base and isolated structures is studied under near-fault ground motions. For this purpose a numerical investigation is carried out by using a step-by-step procedure (Mazza and Vulcano, 2012a and 2012b). At each step of the analysis, plastic conditions are checked at the potential critical sections of the girders and columns using a bilinear model with a hardening ratio of 5%. In order to take into account the plastic deformations along the girders, each of them is discretized into four sub-elements of equal length; in this way, the potential critical sections correspond to end, quarter-span and mid-span sections (see Figures 2b and 4b). In the Rayleigh hypothesis, the damping matrix of the superstructure is assumed as a linear combination of the mass and stiffness matrices: a viscous damping ratio of 5%, for the fixed base structures, and 2%, for all the isolated structures, is assumed in both the horizontal (ξ_H) and vertical (ξ_V) directions with reference to the two vibration periods, T_{1H} and T_{1V}, corresponding to higher-participation modes in the horizontal or vertical direction, respectively.

The local damage undergone by the frame members is evaluated considering the ductility demand calculated in terms of curvature, with reference to the two loading directions, assuming as yielding curvature for the columns the one corresponding to the axial load due to the gravity loads.

The ultimate values of the total shear strain ($\gamma_{tot,u}$) and the corresponding shear strain due to seismic displacement ($\gamma_{s,u}$) of a HDLRB are assumed equal to 7.5(=1.5×5) and 3(=1.5×2), respectively (i.e. 1.5 times the design values); moreover, the compressive and tensile axial loads are limited, respectively, to the critical buckling load (P_{cr}), evaluated according to Eq. (2a), and the tensile value (P_{tu}), obtained multiplying the reduced effective area by a limit stress tension σ_{tu}=0.7 MPa. The sliding friction coefficient μ_F is evaluated for mean values of contact pressure and temperature, e.g. assuming μ_{min}=3%, μ_{max}=15% and α=0.02 s/mm in Eq. (4b).

According to the design hypotheses adopted for the isolated structures (i.e. subsoil class D and high-risk seismic region), accelerograms recorded on soft soil, with a PGA_H value approximately comparable with the one prescribed by NTC08 (PGA_H=0.404g), are considered. More specifically, near-fault ground motions recorded at Taiwan in 1999 (Chi-Chi TCU068 station: E-W and vertical components) and Imperial Valley in 1979 (El Centro D.A. station: horizontal, 360, and vertical components), available in the Pacific Earthquake Engineering Research center database (PEER, 2008), have been considered. It is interesting to note that large horizontal pulses have been observed in the Chi-Chi earthquake; on the other hand, the El Centro D.A. earthquake is characterized by a high value of the acceleration ratio α_{PGA}(=PGA_V/PGA_H).

Firstly, in order to emphasize the effects due to the horizontal and vertical components of near-fault ground motions on the inelastic response of the superstructure, results obtained for the FB five-storey framed structure (see Figure 2a) are compared with those obtained for isolated structures: BI (Figure 5), BIPS (e.g. BIPS-A, Figure 6) and BISS (e.g. BISS-A, Figure 7) structures. To this end, mean ductility demand at all the floor levels is reported for the end-sections (Figures 5a, 6a, 7a: Chi-Chi ground motion) and mid-span sections (Figures 5b, 6b, 7b: El Centro D.A. ground motion) of the girders. For brevity, only the results for the girders of the central frame, having a tributary area for gravity loads greater than those corresponding to the lateral and interior frames (see Figure 2a), are reported for three values of the nominal stiffness ratio α_{K0} of the elastomeric bearings, i.e. 200, 800 and 2000). As shown, the isolation systems were generally effective for reducing damage of the r.c. framed structures, except BIPS system under Chi-Chi motion components (Figure 6a).

It should be noted that the nonlinear dynamic analyses have been stopped at the time t when a limit state is reached: i.e., for the total shear strain of the HDLRBs or the ductility demand of r.c. members (e.g., at the end-sections of the girders, under Chi-Chi motions; at the mid-span sections of the girders, under El Centro D.A. motions). In order to make the results for isolated structures comparable, the analyses have been carried out once again assuming as final instant of simulation, for each ground motion and isolated structure, the minimum one among those before evaluated. The results obtained for Chi-Chi ground motion (Figures 5a, 6a, 7a), characterized by high values of the (horizontal) pseudo-acceleration in the range of rather long vibration periods (i.e. $T_{1H}\geq$2.5 s), have highlighted that unexpected high ductility demands are induced at the lower floors.

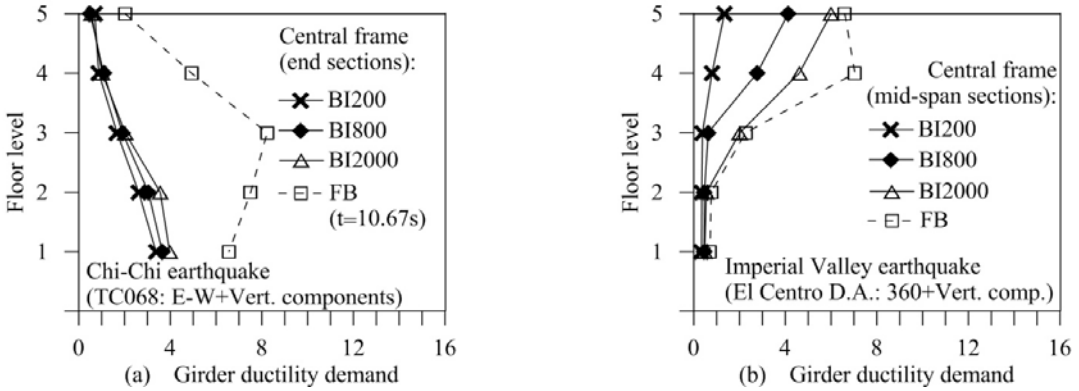

Figure 5. Effects of the nominal stiffness ratio $\alpha_{K0}(=K_{V0}/K_{H0})$ on the ductility demand of girders of BI structures

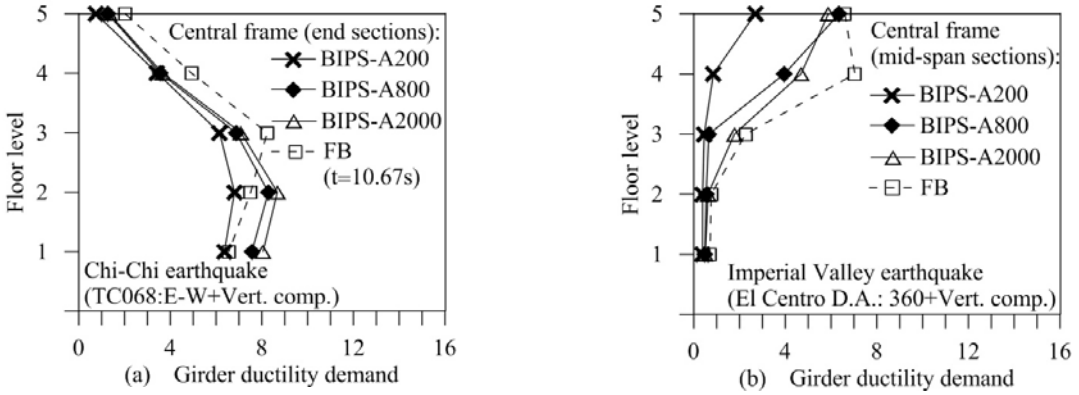

Figure 6. Effects of the nominal stiffness ratio $\alpha_{K0}(=K_{V0}/K_{H0})$ on the ductility demand of girders of BIPS-A structures

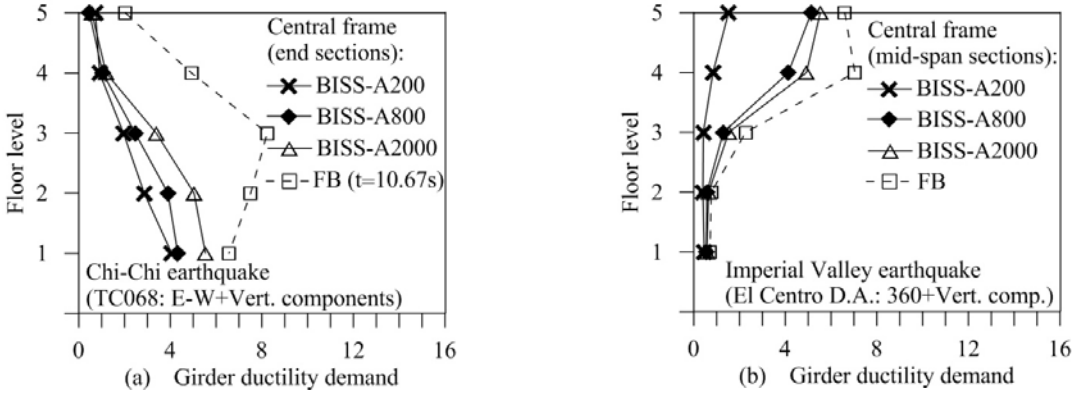

Figure 7. Effects of the nominal stiffness ratio $\alpha_{K0}(=K_{V0}/K_{H0})$ on the ductility demand of girders of BISS-A structures

This result is more evident for BIPS-A structures (especially in Figure 6a), whose behaviour in the horizontal direction is that of a fixed-base structure until the friction threshold imposed by the sliding bearings is not exceeded. Moreover, it is interesting to note, in all cases, a limited influence of α_{K0} value on the ductility demand. As shown in a previous work (Mazza and Vulcano, 2012a and 2012b), the E-W component of Chi-Chi earthquake induces also ductility demand at the end sections of columns, especially at the lower storeys.

On the other hand, under the El Centro D.A. ground motion (Figures 5b, 6b, 7b), characterized by high values of the vertical pseudo-acceleration for rather low values of the vibration periods (i.e.

T_{1V}<0.16 s), the mid-span sections of the girders undergo increasing plastic deformations for an increasing α_{K0} value, especially at the upper floors. This behaviour can be explained observing that for rather low values of α_{K0} (e.g. α_{K0}=200) the superstructure of the BI and BISS-A structures can be considered partially isolated along the vertical direction, exhibiting a basically elastic behaviour, while for rather high values of α_{K0} (e.g. α_{K0}=2000) the same superstructure can be assumed as a fixed-base structure with reference to the same direction. Moreover, a behaviour similar to that of a fixed-base structure is expected in the vertical direction for the BIPS-A structures.

Analogous curves to those shown above for the girders are reported in Figures 8 and 9 to compare the response of the BIPS and BISS isolation systems assuming, for a same value of α_{K0} (i.e. α_{K0}=800), different in-plan layout of elastomeric and sliding bearings (see Figure 3). Curves for BI structure are also reported for a comparison. As regards the ductility demand of the end sections of girders, the results show that for Chi-Chi ground motion (Figures 8a and 9a) both the BIPS and BISS systems have not improved the performance of the superstructure, which becomes even worse of that observed for the BI structure. This is evident for ever-higher values of the nominal sliding ratio α_{S0}(=$F_{S0}/F_{S0,max}$), which are reached when using BIPS systems, because the structural behaviour in the horizontal direction tends to become ever-closer to that of a fixed-base structure. The BISS systems prove to be generally more effective than the BIPS ones for controlling the structural damage of the framed structure, producing elongation of the effective fundamental vibration period, thus limiting the maximum horizontal acceleration transmitted to the superstructure.

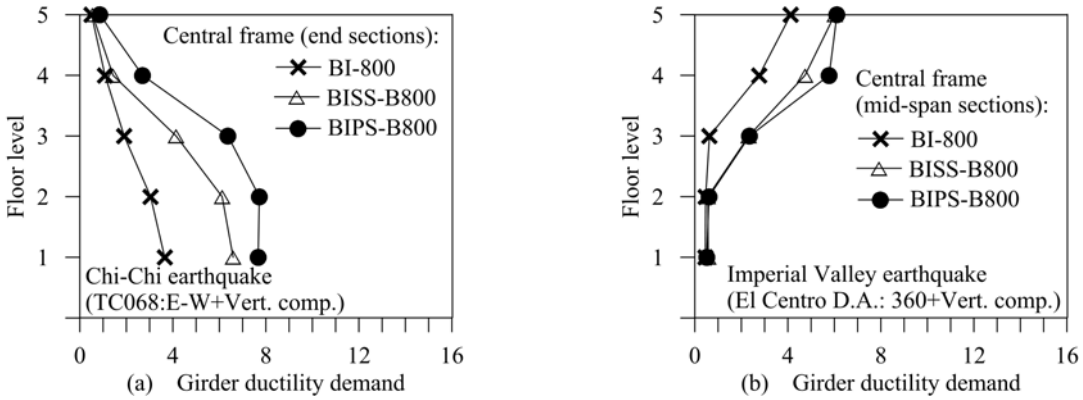

Figure 8. Ductility demand to girders of BI, BISS-B and BIPS-B structures, which exhibit a different nominal sliding ratio α_{S0} (=$F_{S0}/F_{S0,max}$)

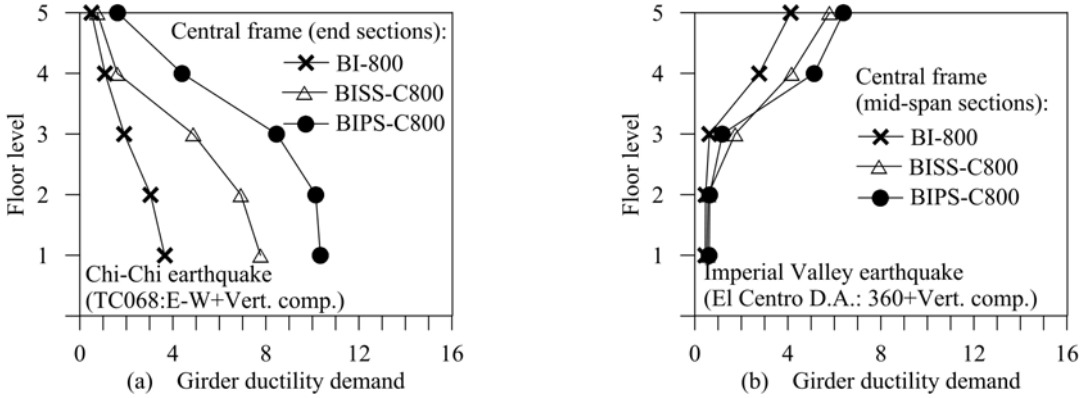

Figure 9. Ductility demand to girders of BI, BISS-C and BIPS-C structures, which exhibit a different nominal sliding ratio α_{S0} (=$F_{S0}/F_{S0,max}$)

Analogous curves for BI, BISS and BIPS structures are shown in Figures 8b and 9b, but reporting ductility demand of the mid-span sections of girders under Imperial Valley ground motion.

As can be observed, the in-plan configuration of elastomeric and sliding bearings turns out to be of little importance, producing only moderate differences in the ductility demand at the upper

floors, where it is still higher than that obtained for the BI structure. Moreover, it is worth noting that the influence of α_{S0} is less evident for El Centro D.A. motion components than for Chi-Chi components. Time histories of the total shear strain for the central isolator of the BI800, BIPS-A800 and BISS-A800 systems subjected to Chi-Chi ground motion, here not reported for brevity, showed that the failure occurs before the end of ground motion, because the limit value $\gamma_{tot,u}$ is exceeded, proving that the BIPS-A800 system is the most favourable to control the isolator displacement.

Moreover, high values of α_{PGA} can notably modify the axial load in r.c. columns and the ductility demand along the span of the girders (Mazza and Vulcano, 2012a and 2012b), while elastomeric and sliding bearings can undergo tensile loads (Kasalanati and Constantinou, 2005) and uplifts (Ryan and Chopra, 2006), respectively.

Finally, the nonlinear dynamic response of the six-storey r.c. framed structures, base-isolated by friction pendulum bearings, is analyzed under the horizontal and vertical components of the Imperial Valley motion (El Centro D.A. station). More specifically, in order to emphasize the influence of the damping ratio ξ, in Figure 10 the maximum ductility demands of deep girders (at the end and quarter-span sections), flat girders (at the end sections) and columns are plotted at all the floor levels.

As can be observed, an increasing value of the equivalent viscous damping at the isolation level does not guarantee a better performance of the superstructure; this happens because a supplemental dissipation at the base results in a reduction of the isolation effectiveness and, as a consequence, in a trend towards a fixed-base behaviour for $\xi_H \to \infty$. Further results, omitted for the sake of brevity, confirmed that the choice of increasing the value of the damping factor, ξ_H, is beneficial to controlling the maximum isolator displacement but it can be unfavourable in terms of residual displacements.

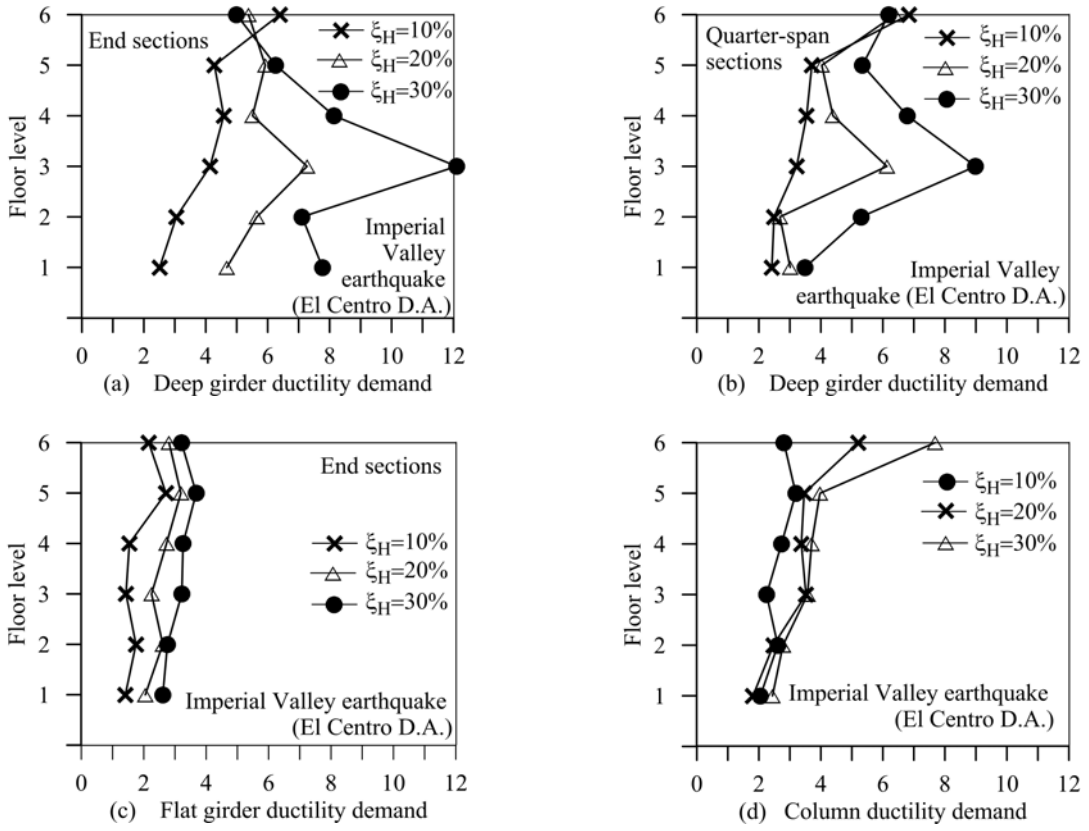

Figure 10. Ductility demand for r.c. frame members of the buildings base-isolated by friction pendulum bearings

CONCLUSIONS

The nonlinear seismic response of fixed-base and base-isolated r.c. framed structures has been studied under near-fault ground motions. Different in-plan layout of elastomeric and sliding bearings has been considered for a five-storey r.c. framed superstructure, assuming different values of the nominal

stiffness ratio α_{K0}, for the HDLRBs, and nominal sliding ratio α_{S0}, for the steel-PTFE sliding plates.

The insertion of an isolation system, except BIPS under Chi-Chi motion components, has been generally beneficial. However, the adoption of BI, BIPS and BISS systems can induce unexpected high ductility demand at the end sections of both girders and columns, especially at the lower floors. This has been more evident for increasing values of α_{S0}, especially when using a BIPS system whose behaviour in the horizontal direction tends to become ever-closer to that of a fixed-base structure.

A high value of the peak vertical acceleration of the ground motion produces ductility demand rather evident at the mid-span sections of the girders, especially in the upper floors when assuming a rather high value of α_{K0} for which the superstructure behaves like a fixed-base structure in the vertical direction. The BIPS system is more effective than the BISS one for controlling the horizontal displacement of the isolation system; both systems can need re-centring after an earthquake in case the restoring force of the HDLRBs does not exceed the friction threshold of the sliding plates corresponding to the α_{S0} value.

Finally, the nonlinear analysis of a six-storey framed structure, base-isolated by friction pendulum bearings and subjected to near-fault ground motions, has been carried out. The results confirmed that a supplemental viscous damping at the base is beneficial to controlling the isolator displacement. But the supplemental damping at the isolation level does not guarantee in all the cases a better performance of the superstructure.

ACKNOWLEDGEMENTS

The present work was financed by RELUIS (italian network of university laboratories of earthquake engineering), according to "Progetto D.P.C. – RELUIS 2014-2016, WP1".

REFERENCES

Braga F, Faggella M, Gigliotti R, Laterza M (2005) "Nonlinear dynamic response of HDRB and hybrid HDRB-friction sliders base isolation systems", *Bulletin of Earthquake Engineering*, 3: 333-353

Calvi GM, Pietra D, Moratti M (2010) "Criteri per la progettazione di dispositivi di isolamento a pendolo scorrevole", *Progettazione Sismica*, 3: 7-30 (in Italian)

Dolce M, Cardone D, Croatto F (2005) "Frictional behaviour of steel-PTFE interfaces for seismic isolation", *Bulletin of Earthquake Engineering*, 3: 75-99

Italian Ministry of the Infrastructures (2008) Technical regulations for the constructions, January 14 (in Italian)

Kasalanati A and Constantinou MC (2005) "Testing and modeling of prestressed isolators", *Journal of Structural Engineering*, 131: 857-866

Kelly JM (1997) Earthquake-Resistant Design with Rubber, Springer-Verlag. Berlin and New York

Legge n. 1684 (1962) Technical regulations for the constructions, with special prescriptions in seismic zones, November 25 (in Italian)

Mazza F and Vulcano A (2009) "Nonlinear response of rc framed buildings with isolation and supplemental damping at the base subjected to near-fault earthquakes", *Journal of Earthquake Engineering*, 13(5): 690-715

Mazza F, Vulcano A, Mazza M (2012a) "Nonlinear dynamic response of rc buildings with different base-isolation systems subjected to horizontal and vertical components of near-fault ground motions", *The Open Construction & Building Technology Journal*, 6: 373-383

Mazza F and Vulcano A (2012b) "Effects of near-fault ground motions on the nonlinear dynamic response of base-isolated r.c. framed buildings", *Earthquake Engineering and Structural Dynamics*, 41: 211-232

Naeim F and Kelly JM (1999) Design of seismic isolated structures: from theory to practice, Wiley & S. Ltd, NY

Pacific Earthquake Engineering Research Center (2008) Next Generation Attenuation (NGA) database, http://peer.berkeley.edu/peer_ground_motion_database

Ryan KL and Chopra AK (2006) "Estimating seismic demands for isolation bearings with building overturning effects", *Journal of Structural Engineering*, 132: 1118-1128

Ryan KL, Kelly JK, Chopra AK (2004) "Experimental observation of axial load effects in isolation bearings", *Procs. 13th World Conference on Earthquake Engineering*, Vancouver, Canada, August 1-6, paper No. 1707